Jpn J Radiol (2015) 33:194–200
DOI 10.1007/s11604-015-0398-1

ORIGINAL ARTICLE

# Different enhancement of the hepatic parenchyma in dynamic CT for patients with normal liver and chronic liver diseases and with the dose of contrast medium based on body surface area

**Gen Koiwahara · Takaharu Tsuda · Megumi Matsuda · Masaaki Hirata · Hiroaki Tanaka · Tomoko Hyodo · Teruhito Kido · Teruhito Mochizuki**

Received: 31 October 2014 / Accepted: 26 January 2015 / Published online: 12 February 2015


**Abstract**
*Purpose* The purpose of this study was to characterize hepatic parenchymal enhancement for normal and diseased liver in dynamic computed tomography (CT) with the dose of contrast medium calculated on the basis of body surface area (BSA).
*Materials and methods* The records of 328 consecutive patients who underwent triple-phase contrast-enhanced CT were retrospectively reviewed. The patients were divided into four groups: normal liver ($n = 125$), chronic hepatitis (CH) ($n = 92$), Child–Pugh grade A liver cirrhosis (LC-A) ($n = 78$), and Child–Pugh grade B liver cirrhosis (LC-B) ($n = 33$). All patients received 22 g I $m^{-2}$ as contrast material, calculated on the basis of BSA. CT values were measured in the region of interest during the pre-contrast, arterial, and portal phases, and the change in the CT value (ΔHU, where HU is Hounsfield units) compared with pre-contrast images was calculated.
*Results* Mean ΔHU for the hepatic parenchyma for the normal liver, CH, LC-A, and LC-B groups during the portal phase was 55.5 ± 11.8 HU, 55.2 ± 12.5 HU, 50.0 ± 13.0 HU, and 43.0 ± 12.7 HU, respectively; generalized estimating equation analysis showed the differences were significant ($p < 0.01$).
*Conclusion* Hepatic parenchymal enhancement during the portal phase decreased as the severity of chronic liver damage increased.

G. Koiwahara (✉) · T. Tsuda · M. Matsuda · M. Hirata · H. Tanaka · T. Kido · T. Mochizuki
Department of Radiology, Ehime University Graduate School of Medicine, 454 Shitukawa, Toon, Ehime 791-0925, Japan
e-mail: gkoiwa@m.ehime-u.ac.jp

T. Hyodo
Department of Radiology, Kinki University Faculty of Medicine, 377-2 Ohno-Higashi, Osaka-Sayama, Osaka 589-8511, Japan

**Keywords** Contrast material · Body surface area (BSA) · Computed tomography (CT) · Cirrhosis · Contrast enhancement

## Introduction

Multiphasic contrast-enhanced CT is an important technique for detecting and characterizing liver tumors. Whereas arterial phase images are important for detection of hypervascular tumors [1], portal phase images are equally crucial for detection of hypovascular tumors [2, 3], for example well-differentiated hepatocellular carcinomas (HCCs) and metastatic tumors. Because sufficient hepatic parenchymal enhancement is necessary to depict hypovascular tumors during the portal phase, many studies have investigated the optimum hepatic parenchymal enhancement. Adequate hepatic enhancement is defined as an increase greater than 50 Hounsfield units (HU) [4]. However, the protocols used for dynamic contrast-enhanced CT and patient selection differ among these studies. In some studies, for example, the dose of contrast material was constant, irrespective of patient body weight, or was calculated on the basis of total body weight. Some studies excluded patients with liver disease whereas others included patients with liver disease. A few studies have reported that insufficient hepatic parenchymal enhancement occurs frequently among patients with liver cirrhosis [5, 6]. The incidence of decreased hepatic parenchymal enhancement among patients with chronic liver injury has yet to be fully evaluated.

In addition to the severity of liver injury, many other factors affect hepatic parenchymal enhancement, for example volume and concentration of the contrast material, the rate of injection, and scanning delay time. The dose of contrast

**Table 1** Patient characteristics

| Characteristic | Normal ($n = 125$) | CH ($n = 92$) | LC-A ($n = 78$) | LC-B ($n = 33$) |
|---|---|---|---|---|
| Age (years)*[1] | 66.2 ± 10.5 | 62.7 ± 10.6 | 66.8 ± 10.5 | 65.0 ± 10.0 |
| Sex (M:F)*[2] | 58:67 | 50:42 | 45:33 | 20:13 |
| Weight (kg)*[3] | 56.2 ± 10.3 | 59.5 ± 10.7 | 58.4 ± 12.1 | 60.0 ± 10.8 |
| BSA ($m^2$)*[4] | 1.561 ± 0.173 | 1.624 ± 0.176 | 1.586 ± 0.178 | 1.604 ± 0.158 |

Mean age, sex, weight, and BSA did not differ significantly among the patient groups. Data are the mean ± standard deviation

*Normal* normal liver, *CH* chronic hepatitis, *LC-A* Child–Pugh grade A liver cirrhosis, *LC-B* Child–Pugh grade B liver cirrhosis, *M* male, *F* female, *BSA* body surface area

*[1] $p = 0.081$; *[2] $p = 0.238$; *[3] $p = 0.090$; *[4] $p = 0.064$

material is particularly critical and is the most important factor affecting hepatic parenchymal enhancement [4]. Historically, the dose of contrast material has been determined on the basis of total body weight (TBW). Recently, however, to reduce patient-to-patient variation in hepatic parenchymal enhancement, studies have calculated the dose of contrast material by using the lean body weight (LBW) or the body surface area (BSA) [7–12].

The purpose of this study was to characterize hepatic parenchymal enhancement among patients with normal liver and patients with chronic liver disease in dynamic CT in which the dose of contrast medium was determined on the basis of BSA and a standard dynamic CT protocol was used.

## Materials and methods

### Patient selection

The requirement for institutional approval and informed consent was waived for this retrospective review of patient records and images. Between August 2012 and December 2012, 524 consecutive patients underwent triple-phase contrast enhanced CT by use of the same protocol. We excluded 196 patients from the study for the following reasons: liver cirrhosis categorized as Child–Pugh grade C ($n = 5$), fatty liver with unenhanced attenuation <45 HU ($n = 11$), numerous metastases ($n = 18$), postoperative effect on hepatic perfusion ($n = 78$), overweight (>89 kg) ($n = 3$), technical failure ($n = 15$), multiple HCC ($n = 5$), portal thrombus ($n = 5$), severe artifacts from the reservoir, stenting, excessive lipiodol accumulation ($n = 4$), markedly abnormal perfusion (arterio-portal shunt, Budd–Chiari syndrome, biliary disease, variable tumors ($n = 33$), liver failure ($n = 15$), and cardiac disease ($n = 4$).

Three-hundred and twenty-eight patients were enrolled and divided into four groups: normal liver ($n = 125$), chronic hepatitis (CH) ($n = 92$), liver cirrhosis categorized as Child–Pugh grade A (LC-A) ($n = 78$), and liver cirrhosis categorized as Child–Pugh grade B (LC-B) ($n = 33$). Chronic liver disease was diagnosed primarily by hepatic biopsy. If biopsy specimens were unavailable, diagnosis was based on imaging and clinical data. Fifty-six biopsy specimens were available for patients with CH, LC-A and LC-B. For 147 of the other cases diagnosis was based on imaging. Patients with no history of liver disease or viral hepatitis, and who had normal liver function on laboratory evaluation were categorized into the normal control group. The distribution of patient characteristics among the four groups is listed in Table 1. The distribution of age ($p = 0.081$, one-way ANOVA), sex ($p = 0.238$, $X^2$ test), weight ($p = 0.090$, one-way ANOVA), and BSA ($p = 0.064$; one-way ANOVA) among the four groups was not statistically significantly different.

### Contrast injection protocol

All patients were administered non-ionic iodinated contrast material containing 300–370 mg I $mL^{-1}$. The contrast material was administered through a 20-gauge intravenous catheter in the antecubital vein by use of a power injector (Stellant D dual flow; Medrad, Osaka, Japan). The dose of contrast material was determined on the basis of BSA by use of the Du Bois' formula: BSA ($m^2$) = 0.007184 × Height (cm)$^{0.725}$ × Weight (kg)$^{0.425}$. All patients were administered 22 g I $m^{-2}$ contrast material over a fixed period of 30 s. Iodine weight administered per BSA in square meters was determined so that the mass of iodine prescribed for a patient with an average BSA of 1.52 $m^2$ (height 160 cm, body weight 55 kg) and that for one with an average body weight of 55 kg were identical [12].

The injection rate and volume were automatically determined based on the BSA.

### Computed tomography examination

CT examination was performed by use of a 256-channel MDCT scanner (Philips Brilliance iCT) with four sections

at a 0.625 × 128 mm detector collimation, table feed speed of 128.64 mm $s^{-1}$, and pitch of 0.804. The gantry rotation time was 0.4 s. The images were displayed as 5-mm-thick sections with no intersection gap between the phase sets. For dynamic CT, pre-contrast images were obtained first, and a bolus of nonionic contrast material was then administered intravenously by use of a power injector at the calculated flow rate. The arterial phase was initiated by using the bolus-trigger technique with a 200-HU threshold; the descending aorta was designated as a region-of-interest (ROI) with an additional start delay of 15 s. The portal and equilibrium phases were started with total delays of 40 and 100 s, respectively, after reaching the trigger threshold.

### Quantitative analysis

For quantitative analysis, CT values at the ROIs were measured by one observer for all patients during the pre-contrast, arterial, portal, and equilibrium phases. The ROIs were the abdominal aorta, hepatic parenchyma, and main trunk of the portal vein. The ROIs of the abdominal aorta were positioned at the same level as the ROIs of main trunk of the portal vein. The ROIs encompassed at least 1 $cm^2$. In the hepatic parenchyma, the ROIs were set at three areas for all patients: two separate areas in the right lobe and one area in the left lobe. The mean attenuation value was calculated for each ROI. Visible hepatic and portal vessels, bile ducts, and potential hepatic lesions were excluded from the ROI measurements to reduce partial volume effects. The change in CT value (ΔHU) was calculated by subtracting the pre-contrast CT value from the value measured for each phase. In addition, to enable comparison of the adequacy of contrast enhancement among the four groups, the contrast enhancement in the hepatic parenchyma during the portal phase was graded as: good (ΔHU > 50 HU), moderate (ΔHU 40–50 HU), and insufficient (ΔHU < 40 HU).

### Statistical analysis

Statistical analysis was performed by use of SPSS version 21 (IBM). We performed generalized estimating equation analysis to evaluate the mean ΔHU of the hepatic parenchyma, aorta, and portal vein, because we measured these during the arterial, portal, and equilibrium phases and there may be correlation among the values obtained [13]. A $p$ value of less than 0.05 indicated a significant difference between the groups.

## Results

Results from quantitative analysis of the mean ΔHU values for the hepatic parenchyma, aorta, and portal vein during each phase among the four groups are summarized in Table 2. Mean ΔHU for the hepatic parenchyma during the portal phase for the normal liver, CH, LC-A, and LC-B groups were: 55.5 ± 11.8 HU, 55.2 ± 12.5 HU, 50.0 ± 13.0 HU, and 43.0 ± 12.7 HU, respectively. According to generalized estimating equation analysis, ΔHU for the hepatic parenchyma during the portal phase was significantly different among the four groups ($p < 0.01$). ΔHU for the hepatic parenchyma decreased as the severity of liver damage increased (Fig. 1). ΔHU for the portal vein during the arterial phase was also significantly different among

**Table 2** Comparison of mean ΔHU for the hepatic parenchyma, aorta, and portal vein

| Structure | Phase | Normal | CH | LC-A | LC-B |
|---|---|---|---|---|---|
| Liver[a] | Arterial | 16.8 ± 8.9 | 14.2 ± 7.5 | 14.1 ± 8.8 | 13.8 ± 6.7 |
| | Portal | 55.5 ± 11.8 | 55.2 ± 12.5 | 50.0 ± 13.0 | 43.0 ± 12.7 |
| | Equilibrium | 39.7 ± 9.3 | 40.8 ± 9.5 | 42.7 ± 9.0 | 42.8 ± 9.3 |
| Aorta | Arterial | 303.7 ± 51.1 | 301.2 ± 46.4 | 294.9 ± 48.9 | 270.7 ± 51.9 |
| | Portal | 122.5 ± 19.8 | 120.4 ± 17.8 | 122.9 ± 22.6 | 116.1 ± 22.5 |
| | Equilibrium | 88.8 ± 12.7 | 85.9 ± 15.7 | 87.6 ± 16.1 | 81.5 ± 16.3 |
| PV[b] | Arterial | 101.0 ± 33.4 | 102.2 ± 31.7 | 89.7 ± 37.7 | 71.2 ± 32.0 |
| | Portal | 147.0 ± 24.0 | 149.7 ± 25.7 | 152.8 ± 29.8 | 139.4 ± 29.2 |
| | Equilibrium | 94.6 ± 15.4 | 94.6 ± 12.1 | 95.5 ± 16.1 | 88.4 ± 18.7 |

Data are the mean ± standard deviation

*CH* chronic hepatitis, *LC-A* Child–Pugh grade A liver cirrhosis, *LC-B* Child–Pugh grade B liver cirrhosis, *Liver* hepatic parenchyma, *PV* portal vein, *HU* Hounsfield unit

[a] In generalized estimating equation analysis, ΔHU for the hepatic parenchyma during the portal phase differed significantly among the four groups ($p < 0.001$)

[b] In generalized estimating equation analysis, ΔHU for the portal vein during the arterial phase also differed significantly among the four groups ($p < 0.001$)

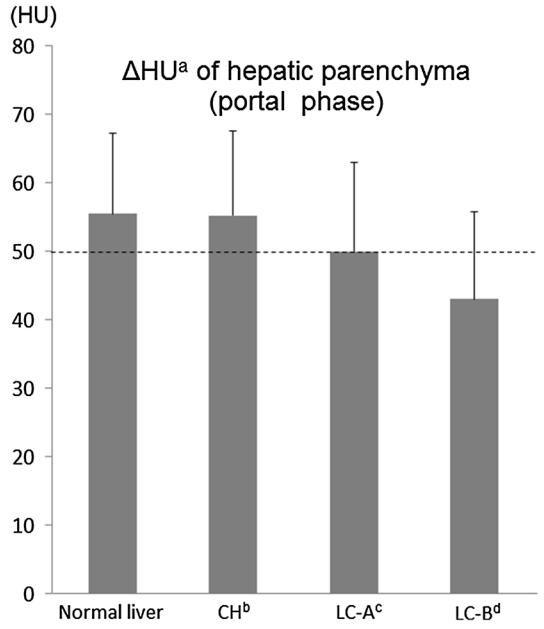


**Fig. 1** ΔHU for the hepatic parenchyma during the portal phase. In generalized estimating equation analysis, ΔHU for the hepatic parenchyma during the portal phase differed significantly among the four groups ($p < 0.01$). ΔHU for the hepatic parenchyma decreased as the severity of liver damage increased. Significance at $p < 0.05$. [a] Hounsfield unit, [b] chronic hepatitis, [c] Child–Pugh grade A liver cirrhosis, [d] Child–Pugh grade B liver cirrhosis. *Error bars* denote 1 standard deviation

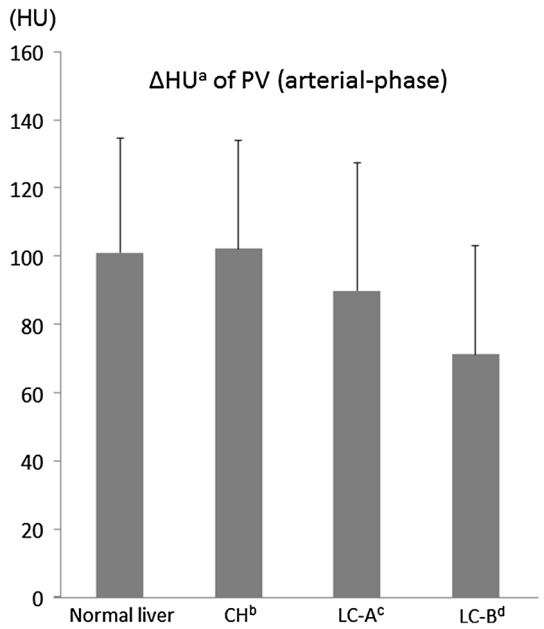


**Fig. 2** ΔHU for the portal vein during the arterial phase. In generalized estimating equation analysis, ΔHU for the portal vein during the arterial phase differed significantly among the four groups ($p < 0.01$). Significance at $p < 0.05$. [a] Hounsfield unit, [b] chronic hepatitis, [c] Child–Pugh grade A liver cirrhosis, [d] Child–Pugh grade B liver cirrhosis. *Error bars* denote 1 standard deviation

**Table 3** Adequacy of contrast enhancement of the hepatic parenchyma during the portal phase

| Enhancement | Normal ($n = 125$) | CH ($n = 92$) | LC-A[a] ($n = 78$) | LC-B[a] ($n = 33$) |
|---|---|---|---|---|
| >50 HU | 83 (66.4 %) | 61 (66.3 %) | 43 (55.1 %) | 12 (36.4 %) |
| 40–50 HU | 30 (24.0 %) | 21 (22.8 %) | 13 (16.7 %) | 6 (18.2 %) |
| <40 HU | 12 (9.6 %) | 10 (10.9 %) | 22 (28.2 %) | 15 (45.4 %) |

Data presented as the number (percentage) of patients

*CH* chronic hepatitis, *LC-A* Child–Pugh grade A liver cirrhosis, *LC-B* Child–Pugh grade B liver cirrhosis, *HU* Hounsfield units

[a] ΔHU for hepatic parenchyma during the portal phase was not adequate for 35 of 78 patients with LC-A or for 21 of 33 patients with LC-B

the four groups ($p < 0.01$). During the arterial phase, ΔHU for the portal vein decreased as the severity of liver damage increased (Fig. 2). Mean ΔHU for the hepatic parenchyma, aorta, and portal vein during the other phases did not differ among the four groups.

The adequacy of hepatic parenchymal enhancement during the portal phase varied within each group (Table 3). In the liver cirrhosis groups, ΔHU for hepatic parenchymal enhancement was adequate (>50 HU) for 43 of 78 patients with LC-A (55.1 %) and for 12 of 33 patients with LC-B (36.4 %). In contrast, for 83 of 125 patients with normal liver (66.4 %) and 61 of 92 patients with CH (66.3 %) ΔHU for hepatic parenchymal enhancement was adequate.

## Discussion

Elevation >50 HU is regarded as the optimum hepatic parenchymal enhancement during the portal phase [14, 15]. Heiken et al. [4] reported that the dose of iodine required to increase hepatic enhancement by 50 HU could be calculated on the basis of the patient's TBW. Recently, several investigators reported that consistent hepatic enhancement could be achieved by calculating the dose of contrast material by using the lean body weight [7, 9] or body surface area (BSA) [8, 10–12] rather than the TBW. In this study, to reduce patient-to-patient enhancement variability, we determined the dose of contrast medium on the basis of BSA. We also used a triple-phase dynamic CT protocol with a fixed duration of injection (30 s) and determined the scanning delay by the bolus-tracking method, which is widely accepted as a standard method [16].

We observed that hepatic parenchymal enhancement was affected by the severity of liver disease. Yanaga et al. [17] reported that 600 mg I $mL^{-1}$ was desirable when evaluating HCC lesions during the portal phase. Several investigators have reported that suboptimum hepatic parenchymal enhancement was frequently observed for patients with

chronic liver diseases [5, 6]. However, studies of different patterns of enhancement of the hepatic parenchyma of the cirrhotic and noncirrhotic liver are uncommon [18–20]. Vignaux et al. [19] performed dynamic contrast-enhanced CT using a single dose (300 mg I $mL^{-1}$, 120 mL) and rate of injection (3 mL $s^{-1}$) of contrast material, irrespective of patient body weight. They compared hepatic parenchymal enhancement from 70 to 95 s after beginning to administer the contrast material by use of dual-detector CT and reported that enhancement during the portal phase was significantly lower for patients with cirrhosis than for those without cirrhosis. Zissen et al. [20] also administered a single dose of contrast material (350 mg I $mL^{-1}$, 150 mL) at a single rate (3 mL $s^{-1}$). They compared hepatic parenchymal enhancement on MDCT 90 s and 10 min after beginning to inject the contrast material. They also reported that the liver-to-aorta enhancement ratio was significantly lower for patients with cirrhosis than for patients without cirrhosis. The timing of the portal phase in these two studies differed from that in ours, because the rate and duration of injection were different. Vignaux et al. compared hepatic enhancement 30–50 s after completion of injection of the contrast materials; Zissen et al. compared images 40 s after completion of injection of the contrast medium. According to Vignaux et al., the duration of injection was 40 s, and hepatic enhancement was maximum after 80–85 s and plateaued from 90–95 s; thus, maximum hepatic enhancement seemed to occur approximately 40 s after the contrast material had been completely injected. Ichikawa et al. [21] reported that the timing of maximum hepatic enhancement mainly depended on the duration of injection and reached a maximum 30 s after completion of injection of the contrast material. Zissen et al. [19] also seemed to select maximum hepatic parenchymal enhancement. The portal phase timing in our study was determined by the bolus-tracking method. As a result, the actual timing of the portal phase was different for each patient. However, the mean timing of the portal phase was approximately 30 s after completion of injection of the contrast material. Thus, our results are consistent with these previous findings and indicate that hepatic parenchymal enhancement in the cirrhotic liver is significantly lower than in the noncirrhotic liver. Moreover, hepatic parenchymal enhancement among patients with Child B liver cirrhosis was lower than among those with Child A type. As the severity of liver cirrhosis increased, hepatic enhancement decreased. However, hepatic parenchymal enhancement during the equilibrium phase was not significantly different between patients with cirrhosis and those without cirrhosis. Partanen [16] reported that the time–density curve for mean contrast enhancement for the liver was similar after 110 s for patients with and without cirrhosis. This trend was attributed to slow wash out of contrast material from the livers of patients with cirrhosis. Hepatic enhancement occurs in two regions, the intravascular space and the extracellular space. The arterial and portal phases are primarily determined by perfusion. For patients with liver cirrhosis, portal hypertension reduces portal perfusion [22–24]. Reduced portal perfusion is compensated by increased arterial perfusion, but our results did not indicate any increase in arterial perfusion. The effect of increased arterial perfusion may be smaller than the effect of reduced portal perfusion during the arterial phase.

We found that enhancement of the portal vein during the arterial phase was significantly lower among patients with liver cirrhosis than among those without liver cirrhosis. This result is similar to those of previous studies [1]. However, there was no significant difference between portal vein enhancement in these two groups during the portal and equilibrium phases. Portal hypertension not only reduces but also delays portal perfusion [19]. During the early phase, CT values mainly reflect the venous return from the splenic and superior mesenteric veins; during the arterial phase, however, portal vein enhancement for the cirrhotic liver simply reflects the delayed portal perfusion. Enhancement of the portal vein itself may not correlate with reduced portal perfusion, because the flow rate and diameter of the portal vein do not necessarily correlate with its CT value. Collateral vasculature may also reduce hepatic enhancement.

Our study showed that optimum hepatic parenchymal enhancement was infrequent among patients with liver cirrhosis. Increasing the dose of contrast material may be an easy solution to this problem. However, a dose increase may be problematic, because this increases the risk of renal toxicity and the cost. The recent emergence of iterative reconstruction methods enables clinicians to perform low-voltage acquisition without increasing image noise. This technique is widely available in current MDCT models and could enable optimum hepatic enhancement without increasing the dose of contrast material [25, 26].

Our study has several limitations. First, we did not use a consistent concentration of contrast material, because the study was conducted in a routine clinical setting. Awai [15] reported there was no significant difference between hepatic enhancement during the portal phase (50 s) and delayed phase (180 s) for moderate and high-concentration protocols. Thus, we assumed variation of the concentration of the contrast material would not significantly affect the results. Second, we defined the portal phase as 40 s after the trigger and the equilibrium phase as 100 s after the trigger. Different timing of the portal and equilibrium phases has been used in previous studies, and the appropriate protocol remains controversial. Mean duration from the start of contrast injection to the trigger was approximately 20 s in our study (data not shown). The portal phase was initiated approximately 60 s after the start of contrast injection

for patients with and without cirrhosis. We did not confirm whether this timing was the maximum hepatic enhancement in our contrast enhancement protocol. Ichikawa et al. [21] reported that time of maximum enhancement of the hepatic parenchyma was the duration of the injection plus 30 s. Their data were generated for patients with HCC, and most also had chronic liver disease. In this study we defined the portal phase with maximum enhancement of the hepatic parenchyma on the basis of these previous data. However, maximum enhancement of the hepatic parenchyma for patients without liver cirrhosis may occur earlier and be higher. Third, we defined the equilibrium phase as the 100-s delay after the trigger; however, this timing may not be the true pharmacologic equilibrium phase [27]. Most studies determine the timing for the equilibrium phase on the basis of the clinical equilibrium phase [28]. In previous studies this phase began at least 90 s after the start of contrast material injection; on the basis of this protocol, our equilibrium phase seems appropriate. Last, diagnosis of liver disease was not always on the basis of liver biopsy. For some patients, diagnosis was based on laboratory, clinical, and imaging data, because histopathological data were unavailable. Although differentiation between chronic liver disease and early liver cirrhosis is difficult, we respect the physician's diagnosis.

In conclusion, hepatic enhancement during the portal phase differed significantly between patients with normal liver and those with chronic liver disease, when a standard injection protocol was used and the dose of contrast material was based on the BSA. The extent of hepatic parenchymal enhancement tended to decrease as the severity of liver damage increased. Suboptimum hepatic parenchymal enhancement was frequent among patients with liver cirrhosis.

**Conflict of interest** The authors declare that they have no conflict of interest.

**Funding** This study was not funded by any entity.

**Informed consent** For this retrospective study the requirement for informed consent was waived by the institutional review board.

**Ethical standard** All procedures performed in studies involving human participants were in accordance with the ethical standards of the institutional and national research committee, and with the 1964 Helsinki declaration and its later amendments or comparable ethical standards.

## References

1. Foley WD, Mallisee TA, Hohenwalter MD, Wilson CR, Quiroz FA, Taylor AJ. Multiphase hepatic CT with a multirow detector CT scanner. AJR Am J Roentgenol. 2000;175:679–85.
2. Haider MA, Amitai MM, Rappaport DC, O'Malley ME, Hanbidge AE, Redston M, et al. Multi-detector row helical CT in preoperative assessment of small (< or = 1.5 cm) liver metastases: is thinner collimation better? Radiology. 2002;225:137–42.
3. Soyer P, Poccard M, Boudiaf M, Abitbol M, Hamzi L, Panis Y, et al. Detection of hypovascular hepatic metastases at triple-phase helical CT: sensitivity of phases and comparison with surgical and histopathologic findings. Radiology. 2004;231:413–20.
4. Heiken JP, Brink JA, McClennan BL, Sagel SS, Crowe TM, Gaines MV. Dynamic incremental CT: effect of volume and concentration of contrast material and patient weight on hepatic enhancement. Radiology. 1995;195:353–7.
5. Awai K, Yagyu Y, W R. Optimal injection protocol in hepatic dynamic CT using MDCT. Jpn J Diagnostic Imaging (In Japanese). 2003;23:1017–25.
6. Furuta A, Ito K, Fujita T, Koike S, Shimizu A, Matsunaga N. Hepatic enhancement in multiphasic contrast-enhanced MDCT: comparison of high- and low-iodine-concentration contrast medium in same patients with chronic liver disease. AJR Am J Roentgenol. 2004;183:157–62.
7. Ho LM, Nelson RC, Delong DM. Determining contrast medium dose and rate on basis of lean body weight: does this strategy improve patient-to-patient uniformity of hepatic enhancement during multi-detector row CT? Radiology. 2007;243:431–7.
8. Bae KT, Seeck BA, Hildebolt CF, Tao C, Zhu F, Kanematsu M, et al. Contrast enhancement in cardiovascular MDCT: effect of body weight, height, body surface area, body mass index, and obesity. AJR Am J Roentgenol. 2008;190:777–84.
9. Kondo H, Kanematsu M, Goshima S, Tomita Y, Kim MJ, Moriyama N, et al. Body size indexes for optimizing iodine dose for aortic and hepatic enhancement at multidetector CT: comparison of total body weight, lean body weight, and blood volume. Radiology. 2010;254:163–9.
10. Yanaga Y, Awai K, Nakaura T, Utsunomiya D, Oda S, Hirai T, et al. Contrast material injection protocol with the dose adjusted to the body surface area for MDCT aortography. AJR Am J Roentgenol. 2010;194:903–8.
11. Onishi H, Murakami T, Kim T, Hori M, Osuga K, Tatsumi M, et al. Abdominal multi-detector row CT: effectiveness of determining contrast medium dose on basis of body surface area. Eur J Radiol. 2011;80:643–7.
12. Kondo H, Kanematsu M, Goshima S, Watanabe H, Kawada H, Moriyama N, et al. Body size indices to determine iodine mass with contrast-enhanced multi-detector computed tomography of the upper abdomen: does body surface area outperform total body weight or lean body weight? Eur Radiol. 2013;23:1855–61.
13. Yanaga Y, Awai K, Nakayama Y, Nakaura T, Tamura Y, Hatemura M, Yamashita Y. Pancreas: patient body weight–tailored contrast material injection protocol versus fixed dose protocol at dynamic CT. Radiology. 2007;245:475–82.
14. Yamashita Y, Komohara Y, Takahashi M, Uchida M, Hayabuchi N, Shimizu T, et al. Abdominal helical CT: evaluation of optimal doses of intravenous contrast material—a prospective randomized study. Radiology. 2000;216:718–23.
15. Awai K, Inoue M, Yagyu Y, Watanabe M, Sano T, Nin S, et al. Moderate versus high concentration of contrast material for aortic and hepatic enhancement and tumor-to-liver contrast at multidetector row CT. Radiology. 2004;233:682–8.
16. Kanematsu M, Goshima S, Kondo H, Nishibori H, Kato H, Yokoyama R, et al. Optimizing scan delays of fixed duration contrast injection in contrast-enhanced biphasic multidetector-row CT for the liver and the detection of hypervascular hepatocellular carcinoma. J Comput Assist Tomogr. 2005;29:195–201.
17. Yanaga Y, Awai K, Nakaura T, Namimoto T, Oda S, Funama Y, et al. Optimal contrast dose for depiction of hypervascular

hepatocellular carcinoma at dynamic CT using 64-MDCT. AJR Am J Roentgenol. 2008;190:1003–9.
18. Partanen KP. Dynamic CT of liver cirrhosis. Invest Radiol. 1984;19:303–8.
19. Vignaux O, Legmann P, Coste J, Hoeffel C, Bonnin A. Cirrhotic liver enhancement on dual-phase helical CT: comparison with noncirrhotic livers in 146 patients. AJR Am J Roentgenol. 1999;173:1193–7.
20. Zissen MH, Wang ZJ, Yee J, Aslam R, Monto A, Yeh BM. Contrast-enhanced CT quantification of the hepatic fractional extracellular space: correlation with diffuse liver disease severity. AJR Am J Roentgenol. 2013;201:1204–10.
21. Ichikawa T, Erturk SM, Araki T. Multiphasic contrast-enhanced multidetector-row CT of liver: contrast-enhancement theory and practical scan protocol with a combination of fixed injection duration and patients' body-weight-tailored dose of contrast material. Eur J Radiol. 2006;58:165–76.
22. Tsushima Y, Blomley JK, Kusano S, Endo K. The portal component of hepatic perfusion measured by dynamic CT: an indicator of hepatic parenchymal damage. Dig Dis Sci. 1999;44:1632–8.
23. Hashimoto K, Murakami T, Dono K, Hori M, Kim T, Kudo M, et al. Assessment of the severity of liver disease and fibrotic change: the usefulness of hepatic CT perfusion imaging. Oncol Rep. 2006;16:677–83.
24. Van Beers BE, Leconte I, Materne R, Smith AM, Jamart J, Horsmans Y. Hepatic perfusion parameters in chronic liver disease: dynamic CT measurements correlated with disease severity. AJR Am J Roentgenol. 2001;176:667–73.
25. Marin D, Nelson RC, Scinbera ST, Richard S, Youngblood RS, Yoshizumi TT, et al. Low-tube-voltage, high-tube-current multidetector abdominal CT: improved image quality and decreased radiation dose with adaptive statistical iterative reconstruction algorithm—initial clinical experience. Radiology. 2010;254:145–53.
26. Shindera ST, Diedrichsen L, Muller HC, Rusch O, Marin D, Schmidt B, et al. Iterative reconstruction algorithm for abdominal multidetector CT at different tube voltages: assessment of diagnostic accuracy, image quality, and radiation dose in a phantom study. Radiology. 2011;260:454–62.
27. Bae KT, Heiken JP, Brink JA. Aortic and hepatic contrast medium enhancement at CT. Part I. Prediction with a computer model. Radiology. 1998;207:647–55.
28. Foley WD. Dynamic hepatic CT. Radiology. 1989;170:617–22.